JACS
JOURNAL OF THE AMERICAN CHEMICAL SOCIETY
Article
pubs.acs.org/JACS

An Intermediate Cobalt(IV) Nitrido Complex and its N-Migratory Insertion Product

Eva M. Zolnhofer,[‡] Martina Käß,[‡] Marat M. Khusniyarov,[‡] Frank W. Heinemann,[‡] Laurent Maron,[∥] Maurice van Gastel,[§] Eckhard Bill,[§] and Karsten Meyer*[,‡]

[‡]Department of Chemistry and Pharmacy, Inorganic Chemistry, Friedrich-Alexander University Erlangen - Nürnberg (FAU), Egerlandstr. 1, 91058 Erlangen, Germany

[∥]Université de Toulouse et CNRS, NSA, UPS, CNRS, UMR 5215 LPCNO, 135 avenue de Rangueil, 31077 Toulouse, France

[§]Max Planck Institute for Chemical Energy Conversion, Stiftstraße 34−36, 45470 Mülheim, Germany

Supporting Information

ABSTRACT: Low-temperature photolysis experiments (T = 10 K) on the tripodal azido complex [(BIMPN^{Mes,Ad,Me})Co^{II}(N_3)] (**1**) were monitored by EPR spectroscopy and support the formation of an exceedingly reactive, high-valent Co nitrido species [(BIMPN^{Mes,Ad,Me})Co^{IV}(N)] (**2**). Density functional theory calculations suggest a low-spin d^5, S = 1/2, electronic configuration of the central cobalt ion in **2** and, thus, are in line with the formulation of complex **2** as a genuine, low-spin Co(IV) nitride species. Although the reactivity of this species precludes handling above 50 K or isolation in the solid state, the N-migratory insertion product [(NH-BIMPN^{Mes,Ad,Me})Co^{II}](BPh$_4$) (**3**) is isolable and was reproducibly synthesized as well as fully characterized, including CHN elemental analysis, paramagnetic ^{1}H NMR, IR, UV−vis, and EPR spectroscopy as well as SQUID magnetization and single-crystal X-ray crystallography studies. A computational analysis of the reaction pathway **2** → **3** indicates that the reaction readily occurs via N-migratory insertion into the Co−C bond (activation barrier of 2.2 kcal mol^{-1}). In addition to the unusual reactivity of the nitride **2**, the resulting divalent cobalt complex **3** is a rare example of a trigonal pyramidal complex with four different donor ligands of a tetradentate chelate—an N-heterocyclic carbene, a phenolate, an imine, and an amine—binding to a high-spin Co(II) ion. This renders complex **3** chiral-at-metal.

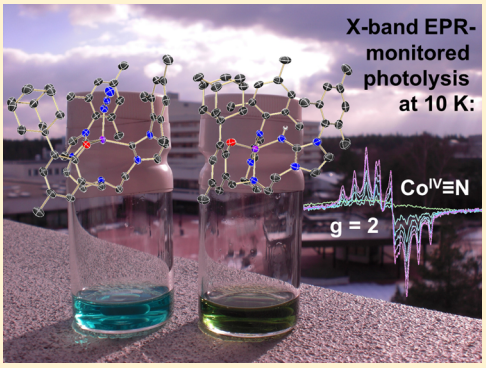

INTRODUCTION

The study of high-valent transition-metal complexes featuring the terminal, multiple bonded oxido (O^{2-}) and nitrido (N^{3-}) ligands is of significant and current interest. This is due to their proposed intermediacy in biological systems and industrial processes[1,2] as well as their application potential in O- and N-atom transfer chemistry in epoxidation and aziridination catalysis.[3−5] For the first-row transition metals manganese and iron, there are a number of structurally characterized mid- to high-valent oxido and nitrido complexes reported in literature.[5−11] In stark contrast, high-valent Co complexes, particularly Co(IV) species, are very rare but have recently attracted increased attention due to their proposed intermediacy in water-splitting catalysis.[12,13]

The reactivity of transition-metal nitrido complexes strongly depends on the number of valence electrons and resulting orbital population of the respective transition metal.[14] Moving from the early to mid- and late first-row transition metals, nonbonding orbitals of the nitrido complexes are filled with electrons until increasingly destabilizing, π-antibonding orbitals have to be occupied. For metal complexes stabilized by a strong π-donor ligand in a tetragonal ligand field, the d-orbitals split into the classic 1 + 2 + 1 + 1 Ballhausen−Gray scheme[15] or, in the limiting case for the more covalent nitrido ligand, in a 1 + 3 + 1 scenario more recently described by Birk and Bendix.[16] Accordingly, exceedingly stable complexes with a maximum of two paired electrons result, such as in low-spin Mn(V) nitrides.[17] An increase in stability of nitrido complexes in a trigonal ligand field is evident from the qualitative orbital splitting diagram of these complexes. In complexes with trigonal symmetry, d(x^2−y^2) is lower in energy, and together with d(xy), represents a set of doubly degenerate, nonbonding orbitals that can be filled with up to four electrons.[18]

Reports on cobalt oxido and nitrido complexes are exceedingly rare,[19−22] and to the best of our knowledge, direct evidence for the existence of a discrete high-valent Co(IV) nitrido complex remains elusive. In 2010, Chirik et al. reported the formation of "putative cobalt nitrido complexes" via photolysis or thermolysis of the corresponding cobalt azide. The secondary products were identified as imine complexes, formed by C−H activation and insertion of the proposed nitrido ligand into a C−H bond of the supporting chelating

Received: August 20, 2014
Published: September 22, 2014

   dx.doi.org/10.1021/ja508144j | J. Am. Chem. Soc. 2014, 136, 15072−15078

ligand. The postulated fleeting nitride intermediate itself was not spectroscopically characterized.[23]

We now report the photolysis of the Co(II) azido complex [(BIMPN^{Mes,Ad,Me})Co^{II}(N$_3$)] (**1**) and the product analysis. Spectroscopic and magnetic characterization as well as computational analyses all support the formation of a discrete but highly reactive Co(IV) nitrido intermediate.

RESULTS AND DISCUSSION

Synthesis. As previously reported, the Co(II) azido precursor, [(BIMPN^{Mes,Ad,Me})Co^{II}(N$_3$)] (**1**), was synthesized by coordinating the tripodal, mixed bis(N-heterocyclic carbene)-mono(phenolate) chelate (BIMPN^{Mes,Ad,Me})$^-$ (Figure 1) to CoCl$_2$, followed by salt metathesis with NaN$_3$.[24]

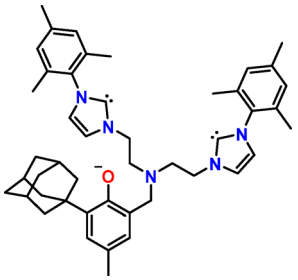

Figure 1. Tripodal mixed bis(carbene)-mono(phenolate) ligand (BIMPN^{Mes,Ad,Me})$^-$ = anion of bis[2-(3-mesityl-imidazol-2-ylidene)-ethyl-(3-adamantyl-2-hydroxy-5-methylphenyl)methyl] amine)].

Photolysis experiments of **1** in solution at room temperature were carried out and optimized to isolate the reaction product. In order to identify the most effective photolysis conditions, temperature and wavelength-dependent photolyses have been carried out from −40 °C to room temperature and over the entire electronic absorption spectrum of **1**, employing a LOT 1000 W Xe-OF arc lamp with a narrow 16 nm window (see SI). These experiments have clearly shown that photolytic azide cleavage exclusively occurs when an absorption band at 310 nm is irradiated; irradiation with other wavelengths has no effect. Furthermore, the photolysis reaction proceeds faster, cleaner, and with better yields if the photolysis is carried out at 310 nm in the presence of a sacrificial hydrogen donor (see SI). Thus, for bulk photolysis, exposure of a blue THF solution of complex **1** and 3 equiv of 2,4,6-tris-*tert*-butylphenol to light of a Heraeus 150 W Hg lamp with near UV light at room temperature facilitates fast conversion to an emerald green solution. Subsequent addition of NaBPh$_4$ allows for the crystallization and isolation of the photolysis product, which was identified as the N-migratory insertion product, namely the monocationic imine complex [(NH-BIMPN^{Mes,Ad,Me})Co^{II}](BPh$_4$) (**3**, see Scheme 1).

Complex **3** was fully characterized, including elemental analysis, paramagnetic ^{1}H NMR, IR, UV−vis, and EPR spectroscopy as well as SQUID magnetization and single-crystal X-ray diffraction studies (see SI). The reaction pathway **1** → **3** was studied by a computational analysis, and the electronic structure was additionally investigated by density functional theory (DFT) calculations (*vide infra*).

Structural Characterization. Single crystals suitable for X-ray diffraction studies were obtained by cooling a concentrated solution of **3** in acetonitrile to −40 °C (Figure 2 and Table 1).

The molecular structure of the cation in **3** shows a four-coordinate Co(II) metal center in a trigonal pyramidal

Scheme 1. Photolysis of the Co(II) Azide 1 and N-Migratory Insertion Reaction of the Transient Cobalt Nitride Complex 2 to yield the Insertion Product 3

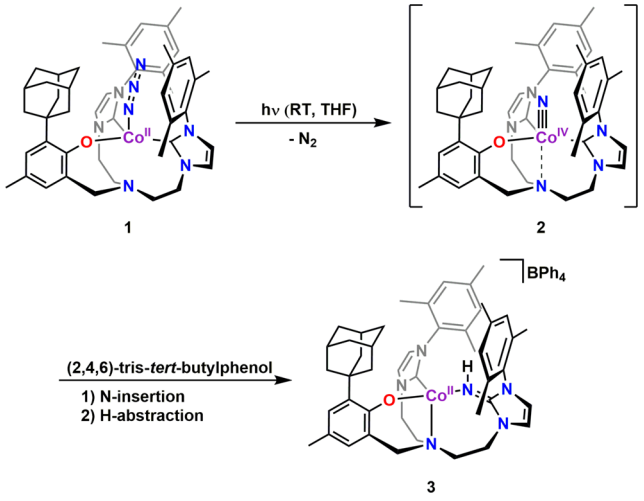

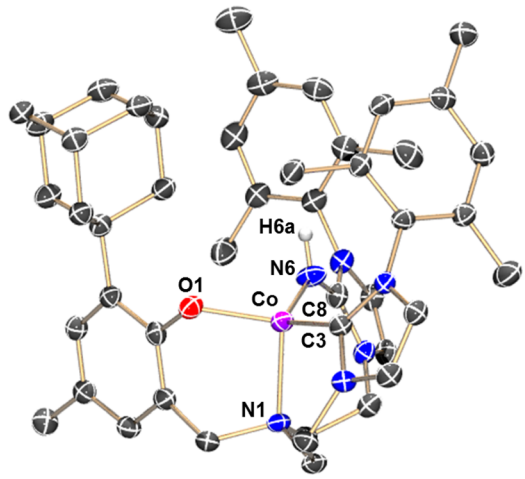

Figure 2. Solid-state molecular structure of the cation of **3** in crystals of [(NH-BIMPN^{Mes,Ad,Me})Co^{II}](BPh$_4$). Thermal ellipsoids are shown at 50% probability; H-atoms, except for the imine-hydrogen, and the BPh$_4^-$ counteranion are omitted for clarity; C, gray, H, white, N, blue, O, red, Co, purple. Only one enantiomer with chiral Co coordination is depicted, whereas the unit cell contains both enantiomers.

Table 1. Selected Bond Distances [Å] and Bond Angles [°] for 3

bond	[Å]	angle	deg
Co−N1	2.106(2)	O1−Co−C3	121.02(9)
Co−O1	1.8927(17)	C3−Co−N6	119.86(10)
Co−C3	2.008(3)	N6−Co−O1	107.24(9)
Co−N6	1.949(2)	N1−Co−O1	97.58(8
N6−H6A	0.8800	N1−Co−C3	97.56(9)
d_{oop}	−0.391	N1−Co−N6	110.04(9)
		Co−N6−C8	133.23(19)

coordination environment. With the molecular structure of the complex cation **3** at hand, the fate of the nitrido ligand in **2** as well as the need for a H donor for complete conversion of **1** becomes obvious: photolysis of **1** evidently leads to a reactive nitrido ligand with a proclivity to insert into one of the two M−C bonds. Subsequent to this N-migratory insertion, H-atom

dx.doi.org/10.1021/ja508144j | J. Am. Chem. Soc. 2014, 136, 15072−15078

abstraction leads to the formation of an imine donor ligand of a new N(amine)-anchored tripodal chelate with four different pendant donors; namely, the anchoring amine N and the original phenolate O, the NHC carbon, plus the newly formed imine N. This renders complex **3** chiral-at-metal. In this ligand environment, the Co center is located −0.391 Å below the trigonal plane, pointing toward the N-anchor. The distance between the N-anchor and the metal center is 2.106(2) Å and considered a bonding interaction, as observed for other N-anchored tripodal carbene and phenolate complexes with one vacant axial coordination site.[24]

Spectroscopy. The ^{1}H NMR spectrum of **3**, recorded either in acetonitrile-d_3 or THF-d_8, reproducibly shows 25 of the 29 expected H resonances for this complex of low symmetry. The remaining signals are likely paramagnetically broadened and shifted and thus not observed. In the IR spectrum of **3**, the intense $\nu_{as}(N_3)$ azide vibrations at 1999, 2081, and 2044 cm^{-1} of starting complex **1** are missing entirely and are replaced by the characteristic but less intense IR vibrations of an imine complex at 3340 cm^{-1} ν(N−H) and 1608 cm^{-1} ν(C═N).

Magnetism. As expected for a divalent Co complex, **3** possesses an S = 3/2 spin ground state, which was experimentally validated by X-band EPR spectroscopy and VT-VH SQUID magnetization measurements (Figure 3) and further confirmed by DFT calculations (see SI). The low-temperature EPR spectrum of **3** at 10 K features a broad, axial-symmetric signal, which was simulated with effective g-values $g_\perp$ = 4.18 and $g_\parallel$ = 2.02. The result is close to the spin-only value expected for the |ms = ±1/2> Kramers doublet of an S = 3/2 system with axial zero-field splitting ($D > h\nu \approx 0.3$ cm^{-1}; $E/D \approx 0$, physical g values: $g_\perp$ = 2.09 and $g_\parallel$ = 2.01). Hyperfine coupling to the ^{59}Co nucleus (I = 7/2, 100%) is not resolved. Complex **3** possesses a magnetic moment, μ_{eff}, of 4.27 μ_B at 300 K, which is due to spin−orbit coupling in Co(II) complexes, higher than the calculated spin-only value of 3.87 μ_B for a high-spin d^7 species with a $^{4}T_{1g}$ ground term.[25] Upon cooling to approximately 50 K, the magnetic moment remains mostly temperature-independent, then gradually decreases to reach a low-temperature moment of μ_{eff} = 3.28 μ_B at 2 K. The observed temperature dependence at T < 50 K is due to zero-field splitting. In order to estimate the magnitude of the zero-field splitting parameter D, field- and temperature-dependent SQUID-measurements of **3** were carried out and simulated to determine |D| to +5.28 cm^{-1} (with g_{ave} = 2.25 and E/D = 0).

The molecular structure of **3**, predicted by DFT calculations for the S = 3/2 state, matches closely the structure obtained from X-ray crystallography (see SI). In contrast, the calculated alternative S = 1/2 state provides metrical parameters that deviate significantly from the experimentally observed ones (see SI). Furthermore, the S = 1/2 spin state is not in agreement with the EPR and SQUID magnetization studies.

The above-mentioned room temperature photolysis of **1** yielding complex **3** via **2** is reminiscent of the reaction of the tris(carbene) Co(I) cation [(TIMEN^{Ar})Co)]$^+$ with organic phenyl azides previously reported by us.[26] In this case, the room temperature reaction of [(TIMEN^{Ar})Co)]$^+$ with R−N$_3$ (with TIMEN^{Ar} = tris[2-(3-aryl-imidazol-2-ylidene)ethyl]-amine; R = −C$_6$H$_4$−CH$_3$, −C$_6$H$_4$−OCH$_3$) yields the corresponding Co(II) bis(carbene) imine complexes via an intermediate Co(III) imido complex, which has been successfully isolated at −35 °C and fully characterized (Scheme 2).

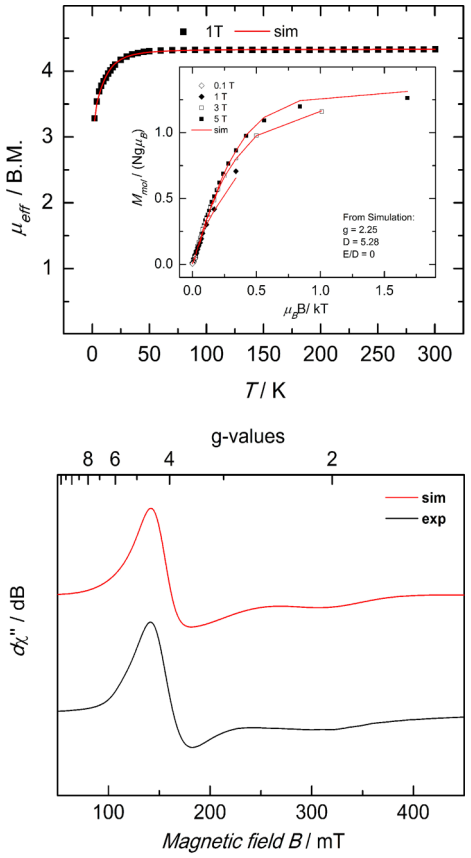

Figure 3. Top: Variable-temperature SQUID magnetization measurements of **3** (χ_{dia} = −731 × 10^{-6} cm^3 mol^{-1}, 1 T, black traces), and their simulations (red traces). Simulation parameters for the field-dependent measurements (inset): S = 3/2, g = 2.25, |D| = +5.28, E/D = 0. Bottom: X-band EPR spectrum of **2** at 10 K, recorded in 1 mM 2-methyl-THF frozen solution (black trace), and its simulation (red trace). Experimental conditions: microwave frequency ν = 8.960 GHz, modulation width = 2.0 mT, microwave power = 2 mW, modulation frequency = 100 kHz, time constant = 0.1 s. Simulation parameters: effective spin S = 1/2, effective g-values $g_\perp$ = 4.18, $g_\parallel$ = 2.02, W_x = 11.6 mT, W_y = 43.5 mT, W_z = 41.1 mT.

Scheme 2. Previously Observed Insertion Reactions of the TIMEN^R (R = 2,6-xylyl, mesityl) Cobalt Imido Complexes[26]

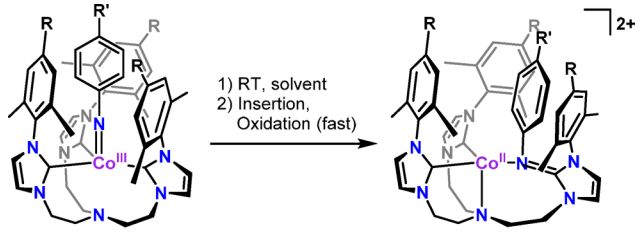

R = H, Me; **R'** = Me, OMe

EPR Spectroscopy of the Transient Nitrido Complex. In an attempt to prove the suggested reaction mechanism and the associated formation of an intermediate Co(IV) nitride species **2**, low-temperature photolysis experiments were carried out *in situ*. Upon irradiation of a frozen sample of **1** at 10 K inside the cryostat of an X-band EPR spectrometer equipped with a JEOL cylindrical cavity with optical access, a new and intense, nearly axial signal at g = 2.01 gradually developed and increased during the time of light exposure. This is the

dx.doi.org/10.1021/ja508144j | J. Am. Chem. Soc. 2014, 136, 15072−15078

predicted signal for an $S = 1/2$ low-spin d^5 cobalt(IV) nitride complex in a trigonal ligand field with a close to 2 + 2 + 1 (or 2 + 1 + 2) d-orbital splitting (Figure 4). In addition, the

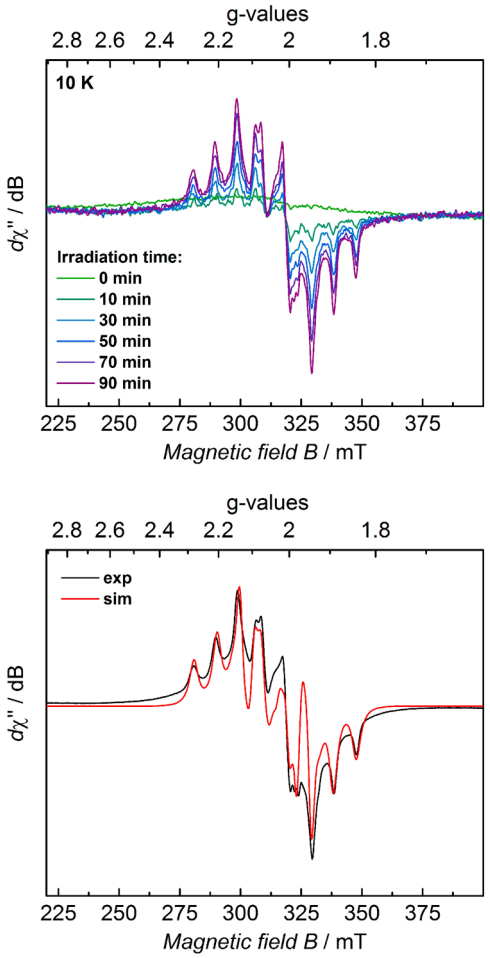

Figure 4. Top: CW X-band EPR-monitored photolysis of **1**, recorded in 1.5 mM 2-methyl-THF frozen solution at 10 K. Experimental conditions: microwave frequency ν = 8.950 GHz, modulation width = 0.5 mT, microwave power = 1 mW, modulation frequency = 100 kHz, time constant = 0.1 s. Bottom: Experimental CW X-band EPR spectrum at 10 K (black trace) and its simulation (red trace). Simulation parameters: $S = 1/2$, $g_1 = 1.99$, $g_2 = 2.09$, $g_3 = 2.04$; $A_{1(Co)}$ = 80 MHz (2.87 mT), $A_{2(Co)}$ = 80 MHz (2.87 mT), $A_{3(Co)}$ = 272 MHz (9.54 mT), and W = 2.1 mT.

highly reproducible EPR signal exhibits an eight-line pattern expected for hyperfine coupling to a ^{59}Co ($I = 7/2$, 100%) nucleus. This observation strongly supports a mechanism with an initial metal-centered, two-electron oxidation of the Co(II) azido complex and formation of a Co(IV) species upon photolysis and subsequent N_2 elimination. Superhyperfine coupling to ^{14}N ($I = 1$, 99.6%), which would provide definite evidence for the coordination of a nitrido ligand, was not observed. The experimentally resolved ^{59}Co hyperfine lines also did not show significant dependence upon sample preparation with ^{15}N azide. However, spectral simulations revealed that the line shapes and widths are compatible with unresolved ^{14}N splitting of about 35 MHz. Hence, solely anisotropic Co coupling with large and small coupling constants was considered in the following EPR analysis (Figure 4). The best simulation to the experimental spectrum was obtained with g-values at $g_1 = 1.99$, $g_2 = 2.09$, $g_3 = 2.04$, a hyperfine coupling with $A_{1(Co)}$ = 80 MHz (2.87 mT), $A_{2(Co)}$ = 80 MHz (2.87 mT), $A_{3(Co)}$ = 272 MHz (9.54 mT), and an isotropic line width of W = 2.1 mT. The data compare well to values reported for other Co(IV) complexes ($g_{iso}/g_{\|} \approx$ 2.00–2.04, $A_{iso(Co)}/A_{\|(Co)}$ = 20–30 G).[27−33]

Temperature-dependent monitoring of the EPR signal at $g \approx 2$ revealed a rapid, gradual decay of the primary photolysis product at liquid-nitrogen temperature (77 K), thus practically excluding the possibility to isolate the transient species or to transfer a photolyzed sample between spectrometers. Due to technical limitations (missing wide-bore optical access for classical light sources or availability of a suitable 300 nm laser) attempts to generate a photolyzed sample of good quality inside one of our cryostats for pulse EPR measurements also failed. This unfortunately prevented us from further probing the superhyperfine coupling of the ^{14}N or ^{15}N isotopomers of **2**. Similarly, and due to the unavailability of He-cooled Raman or IR spectrometers, vibrational spectroscopy at temperatures significantly below 77 K was not possible.

Computation. The molecular and electronic structures of **2** have been further examined by DFT calculations. The molecular structure obtained with BP functional,[34,35] calculated as a spin doublet ($S = 1/2$), reveals two short Co−C (1.91 Å), a moderate Co−O (2.00 Å), and a short C−N (1.59 Å) bond distance in **2**. The corresponding electronic structure has been analyzed by both BP and B3LYP functionals.[36] According to calculations with the BP functional, the spin density is fully delocalized over the Co−$N_{nitride}$ bond, yielding +0.47 and +0.50 spins at the cobalt center and nitrido ligand, respectively (Figure 5). This emphasizes a highly covalent nature of Co−N

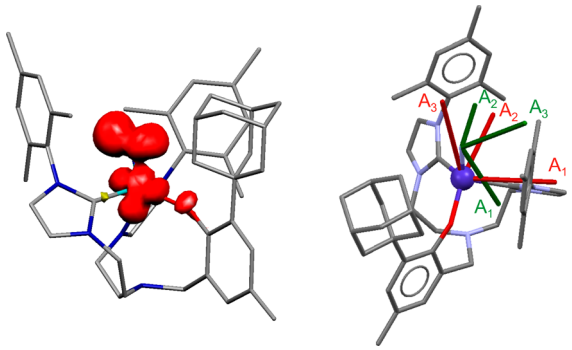

Figure 5. Left: Spin density for **2** ($S = 1/2$) obtained from spin-unrestricted DFT calculations employing the BP functional. Right: Mutual orientation of ^{59}Co (red) and ^{14}N nitride (green) HFC tensors for **2** from spin-unrestricted ZORA-DFT calculations employing the BP functional (for details see SI).

bond. Further analysis of frontier molecular orbitals (MOs) yields five orbitals with significant metal d-character (Figure 6). Two of them are the doubly occupied MOs d(x^2-y^2) and d(xy), d(xz) is a singly occupied orbital (SOMO), whereas d(yz) and d(z^2) remain unoccupied. As usual d(x^2-y^2) and d(xy) are the lowest-lying metal d-orbitals in a quasi-trigonal symmetry.[37] However, due to the loss of C_3 symmetry, the degeneracy of d(x^2-y^2) and d(xy) orbitals is lifted in **2**. The orbital occupation is consistent with a low-spin d^5 $S = 1/2$ electronic configuration of the central metal ion and, thus, in line with the formulation of complex **2** as a genuine, low-spin Co(IV) nitride species.

dx.doi.org/10.1021/ja508144j | J. Am. Chem. Soc. 2014, 136, 15072−15078

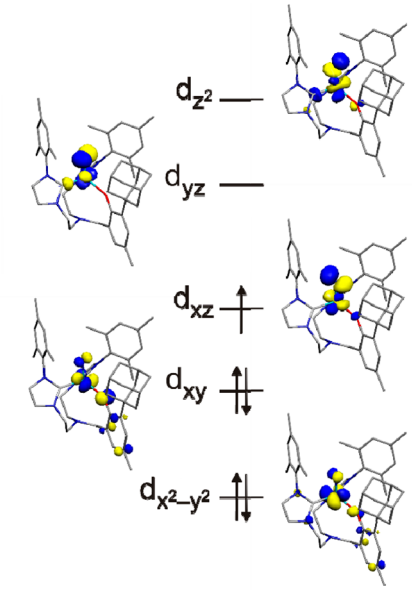

Figure 6. Qualitative molecular orbital diagram for **2** (S = 1/2) obtained from spin-unrestricted DFT calculations employing the BP functional. Quasi-restricted orbitals are shown.

All five metal-based MOs show significant nitrogen contribution. We ascribe this to the highly covalent nature of the Co−N bond in **2**. Note that, due to covalency, a significant amount of spin density is transferred from the cobalt center to the nitrido ligand, which leads to a substantial ligand-based radical character. Although an alternative ground state for the nitride **2** seems highly unlikely, due to unambiguous data from EPR spectroscopy, we calculated the S = 3/2 spin state as well. As expected, the quartet state is higher in energy than the doublet state by 8.4 kcal mol^{-1} (8.2 kcal mol^{-1} after zero point energy corrections) as obtained from calculations with the BP functional. This additionally confirms the S = 1/2 ground state for **2**. Also, the EPR parameters calculated with the BP functional for the S = 1/2 state match the experimentally observed values very well (Table 2). This close match confirms that doublet state obtained from calculations employing the BP functional describes the electronic situation in **2** correctly.[38] Both hyperfine tensors, for ^{59}Co and ^{14}N coupling, show pronounced anisotropy, arising mostly from spin dipole contribution due to anisotropy of the spin density distribution around the cobalt and nitrogen nuclei. Although the largest component of the A^{N} tensor (46 MHz) would exceed the experimental resolution limit of ca. 35 MHz, the DFT results are compatible with the experiment, because the corresponding main axis of the A^{N} tensor is found to be tilted by 71° against the corresponding axis of the A^{Co} tensor, for which the resolved EPR lines have been observed (see SI). This strongly reduces the expected ^{14}N superhyperfine coupling along the direction of the strong 285 MHz ^{59}Co hyperfine coupling below the estimated 35 MHz.

DFT Computational Analysis of Nitride Formation and N-Migratory Insertion. The reaction pathway for this transformation was also computed at the DFT level (see SI). Interestingly, the barrier for N_2 release from [(BIMPN^{Mes,Ad,Me})Co(N_3)], yielding complex **2**, is calculated to be high at 46.8 kcal mol^{-1}; thus, effectively preventing any thermally induced azide-to-nitride transformation but in line with the observed photochemically initiated N_2 elimination from the azido ligand in **1** (Figure 7). The subsequent transformation of **2** to **3**, however, is computed to be spontaneous at room temperature (activation barrier of 2.2 kcal mol^{-1}) and even at temperatures around 80 K (activation barrier of 0.1 kcal mol^{-1}), which is in perfect agreement with the experimental observation. Inspection of the system's SOMO (Figure 8) shows an overlap between the filled nitrido p lone pair and the empty π^* orbital of the carbene (mainly located at the NHC carbon), suggesting that the reaction is a N-migratory insertion into the Co−C_{NHC} bond (or a nucleophilic attack of the terminal nitride to the carbene). It is interesting to note that the latter orbital interaction supports the notion that NHCs are quite potent π-accepting ligands, where the electron density cannot be provided by the high-valent Co ion but from the electron-rich nitride ligand.[39,40]

At the transition state, the nitride N is bridging the Co−C bond, hence supporting the N-migratory insertion type reaction. Following the intrinsic reaction coordinate, this insertion leads (without H-abstraction) to a relatively stable compound that could be formally described as an imido species (Figure 7). However, subsequent H-abstraction yields the imine complex **3** that is even more stable by 35.4 kcal mol^{-1}. Initial H-abstraction from the nitride, to yield the parent imide that subsequently inserts into the M−C bond, seems unlikely because of the exceedingly low activation barrier found for the N-migratory insertion reaction. Indeed, the abstraction would be competitive if the barrier is—at most—similar to the insertion barrier (2.2 kcal/mol). However, such a barrier for a C−H bond activation, even of relatively weak C−H bonds, is unlikely. The barrier for H-abstraction is expected to be around 10 kcal/mol. Accordingly, we suggest that the C−H activation is not competitive with the N-migratory insertion reaction.

Table 2. Calculated and Experimentally Determined EPR Parameters for 2 (S = 1/2)[a]

parameter	DFT	expt
g_1	1.994	1.99
g_2	2.028	2.09
g_3	2.035	2.04
g_{iso}	2.019	–
A_1^{Co}, MHz[b]	−109	80[c]
A_2^{Co}, MHz	+165	80
A_3^{Co}, MHz	+284	272
A_{iso}^{Co}, MHz	+113	–
A_1^{N}, MHz[d]	−18	–
A_2^{N}, MHz	−21	–
A_3^{N}, MHz	+46	–
A_{iso}^{N}, MHz	+2	–

[a]Parameters were obtained from spin-unrestricted ZORA-DFT calculations employing the BP functional. [b]Hyperfine coupling to one ^{59}Co nucleus. [c]The sign of experimentally obtained hyperfine coupling constants have not been determined. [d]Hyperfine coupling to one ^{14}N nitride nucleus. The principal axes of A^{N} are tilted against the coordinates of the g-matrix and A^{Co} tensor. Therefore, the expected hfs along "z" would be less than A_3^{N}. For details see SI.

CONCLUSIONS

In summary, photolysis of the tripodal mixed NHC−phenolate complex [(BIMPN^{Mes,Ad,Me})Co^{II}(N_3)] (**1**) at low temperatures (T = 10 K) generates a transient low-spin Co(IV) nitrido complex. The formation of this S = 1/2 species was followed by EPR spectroscopy, and the molecular and electronic structure

dx.doi.org/10.1021/ja508144j | J. Am. Chem. Soc. 2014, 136, 15072−15078

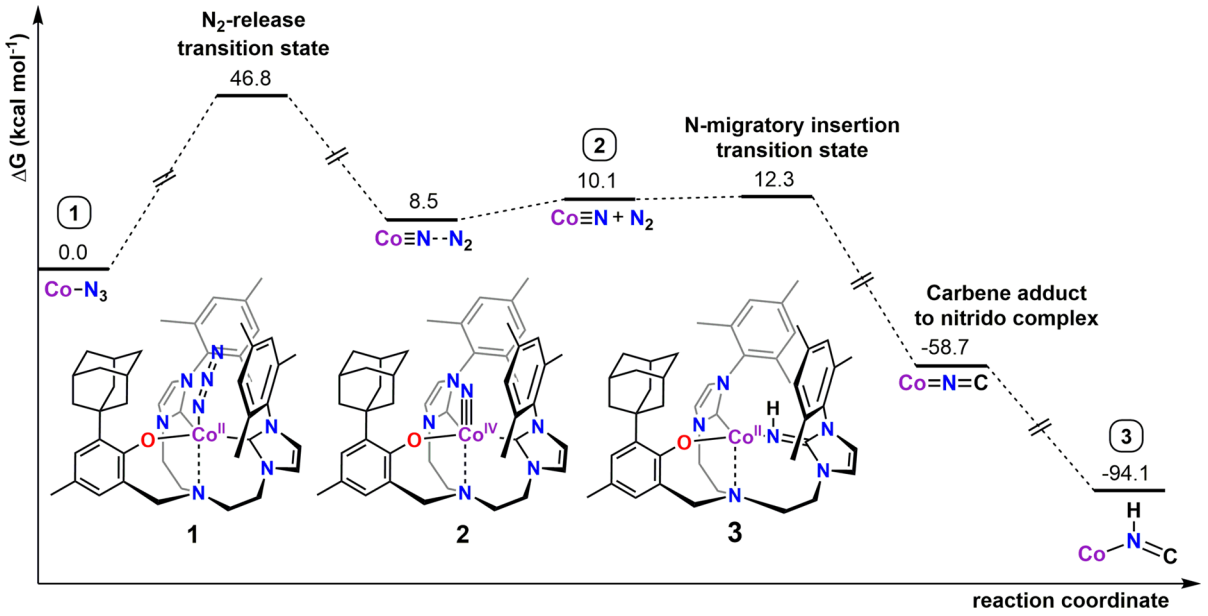

Figure 7. Computed reaction profile for the transformation of azido complex **1** into nitrido complex **2** and the subsequent N-migratory insertion and H-abstraction from **2** to yield the final product, bis(carbene) imine **3**.

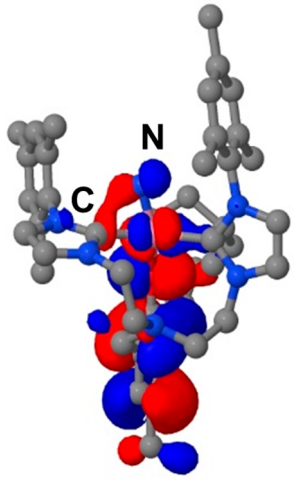

Figure 8. View of the SOMO at the N-migratory insertion transition state (note the carbene−nitride, C−N, orbital interaction).

of this highly reactive complex was studied by DFT computational analysis. At temperatures above 50 K, the nitrido ligand readily inserts into the M−C bond, and subsequent H-abstraction yields a stable cobalt−imine complex. DFT calculations indicate that after photochemical release of N_2 (computed to be kinetically forbidden at room temperature), the formed nitride complex [(BIMPN^{Mes,Ad,Me})-Co^{IV}(N)] (**2**) is undergoing a fast N-migratory insertion into the metal−carbene bond with an activation barrier of only 2.2 kcal/mol. This insertion yields a relatively stable intermediate that subsequently abstracts an H-atom to form the carbene imine phenolate species [(NH-BIMPN^{Mes,Ad,Me})Co^{II}](BPh$_4$) (**3**), which is, together with the N_{amine} anchor, chiral-at-metal. Divalent **3**, synthesized through bulk photolysis of **1** in solution and in the presence of a H donor, was independently isolated on a preparative scale, crystallographically and spectroscopically fully characterized.

■ ASSOCIATED CONTENT

Supporting Information

Synthetic and analytical details, magnetization data, and simulation parameters, and crystallographic details. This material is available free of charge via the Internet at http://pubs.acs.org.

■ AUTHOR INFORMATION

Corresponding Author

karsten.meyer@fau.de

Notes

The authors declare no competing financial interest.

■ ACKNOWLEDGMENTS

We thank the Friedrich-Alexander University Erlangen − Nürnberg (FAU) for financial support. M.M.K. is grateful to the Fonds der Chemischen Industrie and Deutsche Forschungsgemeinschaft for financial support. CalMip is acknowledged for generous grant of computing time. L.M. is a member of the Institut Universitaire de France and acknowledges the Humboldt Foundation. We thank Dr. Susanne Mossin (Technical University of Denmark) for assistance with the simulation of the EPR spectrum of **2**. K.M. acknowledges support of this work by COST Action CM1305 ECOSTBio (Explicit Control Over Spin-States in Technology and Biochemistry).

■ REFERENCES

(1) Eikey, R. A.; Abu-Omar, M. M. *Coord. Chem. Rev.* **2003**, *243*, 83−124.
(2) Berry, J. F. *Comments Inorg. Chem.* **2009**, *30*, 28−66.
(3) Groves, J. T.; Takahashi, T. *J. Am. Chem. Soc.* **1983**, *105*, 2073−2074.
(4) Nugent, W. A.; Mayer, J. M. *Metal-Ligand Multiple Bonds*; John Wiley and Sons: New York, 1988.
(5) Du Bois, J.; Tomooka, C. S.; Hong, J.; Carreira, E. M. *Acc. Chem. Res.* **1997**, *30*, 364−372.
(6) Nam, W. *Acc. Chem. Res.* **2007**, *40*, 522−531.
(7) Que, L. *Acc. Chem. Res.* **2007**, *40*, 493−500.

(8) Saouma, C. T.; Peters, J. C. *Coord. Chem. Rev.* **2011**, *255*, 920−937.
(9) Hohenberger, J.; Ray, K.; Meyer, K. *Nat. Commun.* **2012**, *3*, 720.
(10) Smith, J. M.; Subedi, D. *Dalton Trans.* **2012**, *41*, 1423−1429.
(11) McDonald, A. R.; Que, L., Jr. *Coord. Chem. Rev.* **2013**, *257*, 414−428.
(12) McAlpin, J. G.; Surendranath, Y.; Dincă, M.; Stich, T. A.; Stoian, S. A.; Casey, W. H.; Nocera, D. G.; Britt, R. D. *J. Am. Chem. Soc.* **2010**, *132*, 6882−6883.
(13) Kanan, M. W.; Yano, J.; Surendranath, Y.; Dincă, M.; Yachandra, V. K.; Nocera, D. G. *J. Am. Chem. Soc.* **2010**, *132*, 13692−13701.
(14) Smith, J. M. In *Progress in Inorganic Chemistry*; John Wiley & Sons, Inc.: New York, 2014; Vol *58*, pp 417−470.
(15) Ballhausen, C. J.; Gray, H. B. *Inorg. Chem.* **1962**, *1*, 111−122.
(16) Birk, T.; Bendix, J. *Inorg. Chem.* **2003**, *42*, 7608−7615.
(17) Fleeting intermediates of iron(V) and iron(VI)−nitrido complexes have been spectroscopically characterized but were reported to be exceedingly reactive. See (a) Meyer, K.; Bill, E.; Mienert, B.; Weyhermüller, T.; Wieghardt, K. *J. Am. Chem. Soc.* **1999**, *121*, 4859−4876. (b) Grapperhaus, C. A.; Mienert, B.; Bill, E.; Weyhermüller, T.; Wieghardt, K. *Inorg. Chem.* **2000**, *39*, 5306−5317. (c) Berry, J. F.; Bill, E.; Bothe, E.; George, S. D.; Mienert, B.; Neese, F.; Wieghardt, K. *Science* **2006**, *312*, 1937−1941.
(18) In the case of Peters' tris(phosphino)borate complexes $[(PhBP^{R}_{3})Co^{II}(NR)]$ and $[(PhBP^{R}_{3})Co^{III}(NR)]^{+}$ ($PhBP^{R}_{3}$ = $PhB(CH_2PR_2)_3^-$ with R = Ph, ^{i}Pr), the resulting electronic structure provides a set of three, nearly nonbonding orbitals that can be occupied with up to six electrons. See (a) Jenkins, D. M.; Di Bilio, A. J.; Allen, M. J.; Betley, T. A.; Peters, J. C. *J. Am. Chem. Soc.* **2002**, *124*, 15336−15350. (b) Jenkins, D. M.; Peters, J. C. *J. Am. Chem. Soc.* **2003**, *125*, 11162−11163. (c) Jenkins, D. M.; Peters, J. C. *J. Am. Chem. Soc.* **2005**, *127*, 7148−7165.
(19) Taylor, I. F.; Blanksby, S. J.; Colbran, S. B.; Willett, G. D. *Rapid Commun. Mass Spectrom.* **2010**, *24*, 1142−1146.
(20) Schlangen, M.; Schwarz, H. *Chem. Commun.* **2010**, *46*, 1878−1880.
(21) Pfaff, F. F.; Kundu, S.; Risch, M.; Pandian, S.; Heims, F.; Pryjomska-Ray, I.; Haack, P.; Metzinger, R.; Bill, E.; Dau, H.; Comba, P.; Ray, K. *Angew. Chem., Int. Ed.* **2011**, *50*, 1711−1715.
(22) Hong, S.; Pfaff, F. F.; Kwon, E.; Wang, Y.; Seo, M.-S.; Bill, E.; Ray, K.; Nam, W. *Angew. Chem., Int. Ed.* **2014**, *53*, 10403−10407.
(23) Hojilla, A.; Crisita, C.; Bowman, A. C.; Lobkovsky, E.; Chirik, P. J. *J. Am. Chem. Soc.* **2010**, *132*, 16343−16345.
(24) Käß, M.; Hohenberger, J.; Adelhardt, M.; Zolnhofer, E. M.; Mossin, S.; Heinemann, F. W.; Sutter, J.; Meyer, K. *Inorg. Chem.* **2013**, *3*, 2460−2470.
(25) Figgis, B. N.; Hitchman, M. A. *Ligand-Field Theory and Its Applications*; Wiley-VCH: New York, 2000.
(26) Hu, X.; Meyer, K. *J. Am. Chem. Soc.* **2004**, *126*, 16322−16323.
(27) Halpern, J.; Chan, M. S.; Hanson, J.; Roche, T. S.; Topich, J. A. *J. Am. Chem. Soc.* **1975**, *97*, 1606−1608.
(28) Halpern, J.; Topich, J.; Zamaraev, K. I. *Inorg. Chim. Acta* **1976**, *20*, L21−L24.
(29) Topich, J.; Halpern, J. *Inorg. Chem.* **1979**, *18*, 1339−1343.
(30) Koikawa, M.; Gotoh, M.; Okawa, H.; Kida, S. *J. Chem. Soc. Dalton. Trans.* **1989**, *8*, 1613−1616.
(31) Anson, F. C.; Collins, T. J.; Coots, R. J.; Gipson, S. L.; Richmond, T. G. *J. Am. Chem. Soc.* **1984**, *106*, 5037−5038.
(32) Carpenter, G. B.; Clark, G. S.; Rieger, A. L.; Rieger, P. H.; Sweigart, D. A. *J. Chem. Soc., Dalton Trans.* **1994**, 2903−2910.
(33) Rieger, P. H. *Coord. Chem. Rev.* **1994**, *135*−*136*, 203−286.
(34) Becke, A. D. *Phys. Rev. A* **1988**, *38*, 3098−3100.
(35) Perdew, J. P. *Phys. Rev. B* **1986**, *34*, 7406−7406.
(36) Becke, A. D. *J. Chem. Phys.* **1993**, *98*, 5648−5652.
(37) Scepaniak, J. J.; Vogel, C. S.; Khusniyarov, M. M.; Heinemann, F. W.; Meyer, K.; Smith, J. M. *Science* **2011**, *331*, 1049−1052.
(38) Additionally, the electronic structure of **2** has been analyzed with the B3LYP functional employed by us for the calculation of EPR parameters with great success. See (a) Kropp, H.; King, A. E.; Khusniyarov, M. M.; Heinemann, F. W.; Lancaster, K. M.; DeBeer, S.; Bill, E.; Meyer, K. *J. Am. Chem. Soc.* **2012**, *134*, 15538−15544. (b) Witt, A.; Heinemann, F. W.; Sproules, S.; Khusniyarov, M. M. *Chem.—Eur. J.* **2014**, *20*, 11149−11162. However, due to spin-contamination ($\langle S^2 \rangle$ = 1.13) the B3LYP solution gave EPR parameters that are significantly different from the experimentally obtained values (see SI).
(39) Hu, X.; Tang, Y.; Gantzel, P.; Meyer, K. *Organometallics* **2003**, *22*, 612−614.
(40) Hu, X.; Castro-Rodriguez, I.; Olsen, K.; Meyer, K. *Organometallics* **2004**, *23*, 755−764.